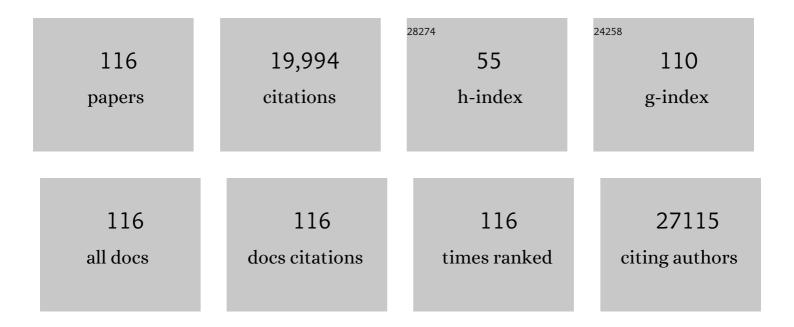
## Judy Cha

## List of Publications by Year in descending order

Source: https://exaly.com/author-pdf/5432878/publications.pdf Version: 2024-02-01



#	Article	IF	CITATIONS
1	Recent Advances in Two-Dimensional Materials beyond Graphene. ACS Nano, 2015, 9, 11509-11539.	14.6	2,069
2	Synthesis of MoS <sub>2</sub> and MoSe <sub>2</sub> Films with Vertically Aligned Layers. Nano Letters, 2013, 13, 1341-1347.	9.1	2,036
3	Hollow Carbon Nanofiber-Encapsulated Sulfur Cathodes for High Specific Capacity Rechargeable Lithium Batteries. Nano Letters, 2011, 11, 4462-4467.	9.1	1,194
4	Self-limited plasmonic welding of silver nanowireÂjunctions. Nature Materials, 2012, 11, 241-249.	27.5	1,002
5	First-row transition metal dichalcogenide catalysts for hydrogen evolution reaction. Energy and Environmental Science, 2013, 6, 3553.	30.8	946
6	Electrochemical tuning of vertically aligned MoS <sub>2</sub> nanofilms and its application in improving hydrogen evolution reaction. Proceedings of the National Academy of Sciences of the United States of America, 2013, 110, 19701-19706.	7.1	894
7	Improving the Performance of Lithium–Sulfur Batteries by Conductive Polymer Coating. ACS Nano, 2011, 5, 9187-9193.	14.6	815
8	Amphiphilic Surface Modification of Hollow Carbon Nanofibers for Improved Cycle Life of Lithium Sulfur Batteries. Nano Letters, 2013, 13, 1265-1270.	9.1	668
9	Electrospun Metal Nanofiber Webs as High-Performance Transparent Electrode. Nano Letters, 2010, 10, 4242-4248.	9.1	660
10	MoSe <sub>2</sub> and WSe <sub>2</sub> Nanofilms with Vertically Aligned Molecular Layers on Curved and Rough Surfaces. Nano Letters, 2013, 13, 3426-3433.	9.1	653
11	New Nanostructured Li <sub>2</sub> S/Silicon Rechargeable Battery with High Specific Energy. Nano Letters, 2010, 10, 1486-1491.	9.1	612
12	High-Mobility Field-Effect Transistors from Large-Area Solution-Grown Aligned C <sub>60</sub> Single Crystals. Journal of the American Chemical Society, 2012, 134, 2760-2765.	13.7	481
13	Dual Tuning of Ni–Co–A (A = P, Se, O) Nanosheets by Anion Substitution and Holey Engineering for Efficient Hydrogen Evolution. Journal of the American Chemical Society, 2018, 140, 5241-5247.	13.7	461
14	Few-Layer Nanoplates of Bi <sub>2</sub> Se <sub>3</sub> and Bi <sub>2</sub> Te <sub>3</sub> with Highly Tunable Chemical Potential. Nano Letters, 2010, 10, 2245-2250.	9.1	403
15	Free-standing nanoparticle superlattice sheets controlled by DNA. Nature Materials, 2009, 8, 519-525.	27.5	372
16	Improving lithium–sulphur batteries through spatial control of sulphur species deposition on a hybrid electrode surface. Nature Communications, 2014, 5, 3943.	12.8	369
17	Ambipolar field effect in the ternary topological insulator (BixSb1–x)2Te3 by composition tuning. Nature Nanotechnology, 2011, 6, 705-709.	31.5	345
18	Rapid Surface Oxidation as a Source of Surface Degradation Factor for Bi <sub>2</sub> Se <sub>3</sub> . ACS Nano, 2011, 5, 4698-4703.	14.6	320

ЈИДУ СНА

#	Article	IF	CITATIONS
19	Topological Insulator Nanowires and Nanoribbons. Nano Letters, 2010, 10, 329-333.	9.1	298
20	Anisotropic Black Phosphorus Synaptic Device for Neuromorphic Applications. Advanced Materials, 2016, 28, 4991-4997.	21.0	281
21	Metal Seed Layer Thickness-Induced Transition From Vertical to Horizontal Growth of MoS <sub>2</sub> and WS <sub>2</sub> . Nano Letters, 2014, 14, 6842-6849.	9.1	251
22	Efficient electrical control of thin-film black phosphorus bandgap. Nature Communications, 2017, 8, 14474.	12.8	249
23	Ultra-low carrier concentration and surface-dominant transport in antimony-doped Bi2Se3 topological insulator nanoribbons. Nature Communications, 2012, 3, 757.	12.8	197
24	Intercalation in two-dimensional transition metal chalcogenides. Inorganic Chemistry Frontiers, 2016, 3, 452-463.	6.0	181
25	Weak Antilocalization in Bi <sub>2</sub> (Se <sub><i>x</i></sub> Te <sub>1–<i>x</i></sub> ) <sub>3</sub> Nanoribbons and Nanoplates. Nano Letters, 2012, 12, 1107-1111.	9.1	166
26	Multifunctional nanoarchitectures from DNA-based ABC monomers. Nature Nanotechnology, 2009, 4, 430-436.	31.5	164
27	One-Step Synthesis of MoS <sub>2</sub> /WS <sub>2</sub> Layered Heterostructures and Catalytic Activity of Defective Transition Metal Dichalcogenide Films. ACS Nano, 2016, 10, 2004-2009.	14.6	164
28	Ultrathin Topological Insulator Bi <sub>2</sub> Se <sub>3</sub> Nanoribbons Exfoliated by Atomic Force Microscopy. Nano Letters, 2010, 10, 3118-3122.	9.1	163
29	Chemical Intercalation of Zerovalent Metals into 2D Layered Bi <sub>2</sub> Se <sub>3</sub> Nanoribbons. Journal of the American Chemical Society, 2012, 134, 13773-13779.	13.7	160
30	High-Density Chemical Intercalation of Zero-Valent Copper into Bi <sub>2</sub> Se <sub>3</sub> Nanoribbons. Journal of the American Chemical Society, 2012, 134, 7584-7587.	13.7	152
31	Strong Metal–Phosphide Interactions in Core–Shell Geometry for Enhanced Electrocatalysis. Nano Letters, 2017, 17, 2057-2063.	9.1	145
32	Highly Conductive, Mechanically Robust, and Electrochemically Inactive TiC/C Nanofiber Scaffold for High-Performance Silicon Anode Batteries. ACS Nano, 2011, 5, 8346-8351.	14.6	122
33	Topological nanomaterials. Nature Reviews Materials, 2019, 4, 479-496.	48.7	122
34	Magnetic Doping and Kondo Effect in Bi <sub>2</sub> Se <sub>3</sub> Nanoribbons. Nano Letters, 2010, 10, 1076-1081.	9.1	119
35	One-Dimensional Helical Transport in Topological Insulator Nanowire Interferometers. Nano Letters, 2014, 14, 2815-2821.	9.1	118
36	Emulating Bilingual Synaptic Response Using a Junction-Based Artificial Synaptic Device. ACS Nano, 2017. 11. 7156-7163.	14.6	106

#	Article	IF	CITATIONS
37	Effective Interlayer Engineering of Two-Dimensional VOPO <sub>4</sub> Nanosheets via Controlled Organic Intercalation for Improving Alkali Ion Storage. Nano Letters, 2017, 17, 6273-6279.	9.1	102
38	Optical transmission enhacement through chemically tuned two-dimensional bismuth chalcogenide nanoplates. Nature Communications, 2014, 5, 5670.	12.8	99
39	Ultrathin dendrimer–graphene oxide composite film for stable cycling lithium–sulfur batteries. Proceedings of the National Academy of Sciences of the United States of America, 2017, 114, 3578-3583.	7.1	90
40	Low Reflectivity and High Flexibility of Tin-Doped Indium Oxide Nanofiber Transparent Electrodes. Journal of the American Chemical Society, 2011, 133, 27-29.	13.7	88
41	Direct Synthesis of Large‣cale WTe <sub>2</sub> Thin Films with Low Thermal Conductivity. Advanced Functional Materials, 2017, 27, 1605928.	14.9	86
42	Revealing the Contribution of Individual Factors to Hydrogen Evolution Reaction Catalytic Activity. Advanced Materials, 2018, 30, e1706076.	21.0	86
43	Synthesis of Crystalline Black Phosphorus Thin Film on Sapphire. Advanced Materials, 2018, 30, 1703748.	21.0	86
44	Stepwise Sulfurization from MoO <sub>3</sub> to MoS <sub>2</sub> via Chemical Vapor Deposition. ACS Applied Nano Materials, 2018, 1, 5655-5661.	5.0	86
45	Synthesis of SnTe Nanoplates with {100} and {111} Surfaces. Nano Letters, 2014, 14, 4183-4188.	9.1	75
46	Nano-structured textiles as high-performance aqueous cathodes for microbial fuel cells. Energy and Environmental Science, 2011, 4, 1293.	30.8	72
47	DNAsomes: Multifunctional DNAâ€Based Nanocarriers. Small, 2011, 7, 74-78.	10.0	71
48	Chemically Synthesized Heterostructures of Two-Dimensional Molybdenum/Tungsten-Based Dichalcogenides with Vertically Aligned Layers. ACS Nano, 2014, 8, 9550-9557.	14.6	70
49	A Highly Efficient Allâ€Solidâ€State Lithium/Electrolyte Interface Induced by an Energetic Reaction. Angewandte Chemie - International Edition, 2020, 59, 14003-14008.	13.8	70
50	Selfâ€Healing of a Confined Phase Change Memory Device with a Metallic Surfactant Layer. Advanced Materials, 2018, 30, 1705587.	21.0	69
51	Topological insulator nanostructures. Physica Status Solidi - Rapid Research Letters, 2013, 7, 15-25.	2.4	68
52	Nanoscale size effects in crystallization of metallic glass nanorods. Nature Communications, 2015, 6, 8157.	12.8	65
53	Two-Dimensional Chalcogenide Nanoplates as Tunable Metamaterials via Chemical Intercalation. Nano Letters, 2013, 13, 5913-5918.	9.1	64
54	Functionalization of silicon nanowire surfaces with metal-organic frameworks. Nano Research, 2012, 5, 109-116.	10.4	63

Judy Cha

#	Article	IF	CITATIONS
55	Effects of Magnetic Doping on Weak Antilocalization in Narrow Bi <sub>2</sub> Se <sub>3</sub> Nanoribbons. Nano Letters, 2012, 12, 4355-4359.	9.1	59
56	Unveiling the Interfacial Effects for Enhanced Hydrogen Evolution Reaction on MoS <sub>2</sub> /WTe <sub>2</sub> Hybrid Structures. Small, 2019, 15, e1900078.	10.0	58
57	Ambipolar Field Effect in Sb-Doped Bi <sub>2</sub> Se <sub>3</sub> Nanoplates by Solvothermal Synthesis. Nano Letters, 2013, 13, 632-636.	9.1	57
58	Self-Healing of a Confined Phase Change Memory Device with a Metallic Surfactant Layer. Microscopy and Microanalysis, 2019, 25, 1870-1871.	0.4	56
59	<i>In Situ</i> Transmission Electron Microscopy Observation of Nanostructural Changes in Phase-Change Memory. ACS Nano, 2011, 5, 2742-2748.	14.6	48
60	Revealing Surface States in In-Doped SnTe Nanoplates with Low Bulk Mobility. Nano Letters, 2015, 15, 3827-3832.	9.1	48
61	Suppression of Magnetoresistance in Thin WTe <sub>2</sub> Flakes by Surface Oxidation. ACS Applied Materials & Interfaces, 2017, 9, 23175-23180.	8.0	47
62	Materials for interconnects. MRS Bulletin, 2021, 46, 959-966.	3.5	33
63	Topological crystalline insulator nanostructures. Nanoscale, 2014, 6, 14133-14140.	5.6	32
64	Three-Dimensional Imaging of Carbon Nanotubes Deformed by Metal Islands. Nano Letters, 2007, 7, 3770-3773.	9.1	31
65	Tailoring crystallization phases in metallic glass nanorods via nucleus starvation. Nature Communications, 2017, 8, 1980.	12.8	31
66	General Facet-Controlled Synthesis of Single-Crystalline {010}-Oriented LiMPO <sub>4</sub> (M = Mn,) Tj ETQq(	0.0 rgBT 6.7	/Overlock 10
67	Supercluster-coupled crystal growth in metallic glass forming liquids. Nature Communications, 2019, 10, 915.	12.8	30
68	Recent progress on in situ characterizations of electrochemically intercalated transition metal dichalcogenides. Nano Research, 2019, 12, 2126-2139.	10.4	29
69	The development of 2D materials for electrochemical energy applications: A mechanistic approach. APL Materials, 2019, 7, .	5.1	28
70	cm <sup>2</sup> -Scale Synthesis of MoTe <sub>2</sub> Thin Films with Large Grains and Layer Control. ACS Nano, 2021, 15, 410-418.	14.6	27
71	One Nanometer Resolution Electrical Probe via Atomic Metal Filament Formation. Nano Letters, 2011, 11, 231-235.	9.1	25

72Synergistic Integration of Chemoâ€Resistive and SERS Sensing for Labelâ€Free Multiplex Gas Detection.<br/>Advanced Materials, 2021, 33, e2105199.21.025

#	Article	IF	CITATIONS
73	Surface effects on electronic transport of 2D chalcogenide thin films and nanostructures. Nano Convergence, 2014, 1, 18.	12.1	24
74	Stable Water Oxidation in Acid Using Manganese-Modified TiO <sub>2</sub> Protective Coatings. ACS Applied Materials & Interfaces, 2018, 10, 18805-18815.	8.0	24
75	Semipolar (202Ì1Ì) GaN and InGaN Light-Emitting Diodes Grown on Sapphire. ACS Applied Materials & Interfaces, 2017, 9, 14088-14092.	8.0	23
76	High magnetoresistance tunnel junctions with Mg–B–O barriers and Ni–Fe–B free electrodes. Applied Physics Letters, 2009, 94, 112504.	3.3	22
77	Synthesis of WTe <sub>2</sub> Nanowires with Increased Electron Scattering. ACS Nano, 2019, 13, 6455-6460.	14.6	22
78	The surface surfaces. Nature Nanotechnology, 2012, 7, 85-86.	31.5	21
79	General Nanomolding of Ordered Phases. Physical Review Letters, 2020, 124, 036102.	7.8	21
80	Highly Conductive Single-Walled Carbon Nanotube Thin Film Preparation by Direct Alignment on Substrates from Water Dispersions. Langmuir, 2015, 31, 1155-1163.	3.5	18
81	Formation and stability of complex metallic phases including quasicrystals explored through combinatorial methods. Scientific Reports, 2019, 9, 7136.	3.3	17
82	Heterointerface Effects on Lithium-Induced Phase Transitions in Intercalated MoS <sub>2</sub> . ACS Applied Materials & Interfaces, 2021, 13, 10603-10611.	8.0	17
83	Josephson detection of time-reversal symmetry broken superconductivity in SnTe nanowires. Npj Quantum Materials, 2021, 6, .	5.2	16
84	Nearâ€Unity Molecular Doping Efficiency in Monolayer MoS <sub>2</sub> . Advanced Electronic Materials, 2021, 7, 2000873.	5.1	16
85	Axial Higgs mode detected by quantum pathway interference in RTe3. Nature, 2022, 606, 896-901.	27.8	14
86	Revisiting Intercalationâ€Induced Phase Transitions in 2D Group VI Transition Metal Dichalcogenides. Advanced Energy and Sustainability Research, 2021, 2, 2100027.	5.8	13
87	Unconventional grain growth suppression in oxygen-rich metal oxide nanoribbons. Science Advances, 2021, 7, eabh2012.	10.3	12
88	Surface Functionalization for Magnetic Property Tuning of Nonmagnetic 2D Materials. Advanced Materials Interfaces, 2022, 9, .	3.7	12
89	Synthesis and superconductivity of In-doped SnTe nanostructures. APL Materials, 2017, 5, .	5.1	11
90	Synthesis and resistivity of topological metal MoP nanostructures. APL Materials, 2020, 8, .	5.1	11

#	Article	IF	CITATIONS
91	Crossover between weak antilocalization and weak localization in few-layer <mml:math xmlns:mml="http://www.w3.org/1998/Math/MathML"&gt;<mml:mi mathvariant="normal"&gt;W<mml:msub><mml:mi>Te</mml:mi><mml:mn>2</mml:mn></mml:msub>: Role of electron-electron interactions. Physical Review B, 2020, 102, .</mml:mi </mml:math 	ı <mark>3,2</mark> ıml:math>	11
92	Seeing Quantum Materials with Cryogenic Transmission Electron Microscopy. Nano Letters, 2021, 21, 5449-5452.	9.1	11
93	Synthesis of Narrow SnTe Nanowires Using Alloy Nanoparticles. ACS Applied Electronic Materials, 2021, 3, 184-191.	4.3	10
94	Structural Phase Transition and Carrier Density Tuning in SnSe <i><sub>x</sub></i> Te <sub>1â€</sub> <i><sub>x</sub></i> Nanoplates. Advanced Electronic Materials, 2016, 2, 1600144.	5.1	8
95	Dislocation-driven SnTe surface defects during chemical vapor deposition growth. Journal of Physics and Chemistry of Solids, 2019, 128, 351-359.	4.0	8
96	1D topological systems for next-generation electronics. Matter, 2021, 4, 2596-2598.	10.0	8
97	Thickness-dependent phase transition kinetics in lithium-intercalated MoS <sub>2</sub> . 2D Materials, 2022, 9, 025009.	4.4	8
98	Compact Super Electron-Donor to Monolayer MoS <sub>2</sub> . Nano Letters, 2022, 22, 4501-4508.	9.1	8
99	Heterointerface Control over Lithium-Induced Phase Transitions in MoS <sub>2</sub> Nanosheets: Implications for Nanoscaled Energy Materials. ACS Applied Nano Materials, 2021, 4, 14105-14114.	5.0	7
100	A Gapped Phase in Semimetallic T <sub>d</sub> â€WTe <sub>2</sub> Induced by Lithium Intercalation. Advanced Materials, 2022, 34, e2200861.	21.0	7
101	Direct Observation Through In Situ Transmission Electron Microscope of Early States of Crystallization in Nanoscale Metallic Glasses. Jom, 2017, 69, 2187-2191.	1.9	6
102	The Effect of Mechanical Strain on Lithium Staging in Graphene. Advanced Electronic Materials, 2021, 7, 2000981.	5.1	6
103	Nanoscale Size Effects on Crystallization Kinetics of Metallic Glass Nanorods by In Situ TEM. Microscopy and Microanalysis, 2016, 22, 768-769.	0.4	5
104	Thickness dependence of magnetotransport properties of tungsten ditelluride. Physical Review B, 2021, 104, .	3.2	4
105	Effects of growth substrate on the nucleation of monolayer MoTe <sub>2</sub> . CrystEngComm, 2021, 23, 7963-7969.	2.6	3
106	Surface characterization of ultrathin atomic layer deposited molybdenum oxide films using high-sensitivity low-energy ion scattering. Journal of Vacuum Science and Technology A: Vacuum, Surfaces and Films, 2021, 39, .	2.1	3
107	Spatially resolved In and As distributions in InGaAs/GaP and InGaAs/GaAs quantum dot systems. Nanotechnology, 2014, 25, 465702.	2.6	2
108	Structure-Transport Properties of Topological Nanowires. Microscopy and Microanalysis, 2021, 27, 920-921.	0.4	1

#	Article	IF	CITATIONS
109	Angstrom-scale replication of surfaces with crystallized bulk metallic glasses. Materials Today Nano, 2021, 16, 100145.	4.6	1
110	Synergistic Integration of Chemoâ€Resistive and SERS Sensing for Labelâ€Free Multiplex Gas Detection (Adv. Mater. 44/2021). Advanced Materials, 2021, 33, 2170350.	21.0	1
111	Stackable nonvolatile memory with ultra thin polysilicon film and low-leakage (Ti,Dy)xOy for low processing temperature and low operating voltages. Microelectronic Engineering, 2011, 88, 3462-3465.	2.4	0
112	Tunable Plasmon and Optical Properties of Chalcogenide Nanoplates Using Monochromated Electron Energy Loss Spectroscopy. Microscopy and Microanalysis, 2014, 20, 574-575.	0.4	0
113	Spatially resolved In and As distributions in InGaAs/GaP and InGaAs/GaAs quantum dot systems. Microscopy and Microanalysis, 2014, 20, 614-615.	0.4	0
114	Microscopy and Chemical Analysis of Topological Insulator Bi2Se3 and Topological Crystalline Insulator SnTe Nanostructures. Microscopy and Microanalysis, 2015, 21, 1535-1536.	0.4	0
115	Supercluster-Coupled Crystal Growth in Metallic Glass Forming Liquids. Microscopy and Microanalysis, 2019, 25, 1410-1411.	0.4	0
116	Structure-Property Relationships of Topological Insulator Nanomaterials. Microscopy and Microanalysis, 2019, 25, 962-963.	0.4	0